Molecular Catalysis 457 (2018) 1–7

Contents lists available at ScienceDirect

Molecular Catalysis

journal homepage: www.elsevier.com/locate/mcat

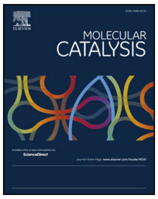

Tuning of oxygen species and active Pd^{2+} species of supported catalysts via morphology and Mn doping in oxidative carbonylation of phenol

Xiaojun Yang[a,b], Yue Hu[a], Hang Bai[a], Maoqi Feng[c], Zhiguo Yan[a,*], Shuo Cao[a,*], Bin Yang[b,*]

[a] Key Laboratory for Green Chemical Process of Ministry of Education, School of Chemical Engineering and Pharmacy, Wuhan Institute of Technology, Wuhan 430205, PR China
[b] Bioproduct Sciences and Engineering Laboratory, Department of Biological Systems Engineering, Washington State University, Richland, WA 99354, USA
[c] Chemistry & Chemical Engineering Division, Southwest Research Institute, San Antonio, TX 78238, USA

ARTICLE INFO

Keywords:
Morphology
Dopants
Oxygen species
Oxidative carbonylation
Ceria

ABSTRACT

A series of nanocubes and nanorods of CeO_2 and Mn_xCe_yO (x,y = 1 or 3) oxides were prepared by the hydrothermal method. Samples as prepared were characterized by Transmission electron microscopy, X-ray diffraction, X-ray photoelectron spectroscopy and Raman spectroscopy, in order to gain a fundamental understanding of the effects of the morphology and Mn dopant on the oxygen species and active Pd^{2+} species in the oxidative carbonylation of phenol using Pd catalysts supported on as-prepared oxides. Although the oxygen species on supports with different morphologies varied, the catalytic performance in the oxidative carbonylation reaction did not show the significant change. Comparatively speaking, the doping of Mn is a more efficient method to control active oxygen species. It is deduced that Pd and Mn are "dopants" for pure CeO_2, both of which improve the formation of oxygen vacancies that help to mitigate the reduction of active Pd species due to the strong interaction between the Pd^{2+} and the Mn_xCe_yO support. Furthermore, we propose that O_β (hydroxyl oxygen, chemisorbed oxygen or the oxygen vacancy) species acted as intermediates to lower the reduction of active palladium species by the strong interaction between the noble metal and supports, while the lattice oxygen O_α were involved in the redox cycle of Pd^0/Pd^{2+} in the oxidative carbonylation of phenol to diphenyl carbonate. All results suggest that Mn dopants play a more important role in the activity than morphology does.

1. Introduction

Diphenyl carbonate (DPC) can be utilized to synthesize many important organic compounds and polymer materials [1,2]. For example, DPC reacts with bisphenol-A to produce polycarbonate, which is widely employed as an engineering plastic. The synthesis of DPC includes the traditional phosgene method, the transesterification process of phenol and aliphatic carbonate, and the oxidative carbonylation of phenol [3,4]. Among them, the oxidative carbonylation of phenol to produce DPC has gained more and more attention due to more stringent environmental policy all over the world [5]. Phenol reacts with CO and O_2, as shown in Eq. (1), to produce DPC and water in the presence of palladium catalysts. During this process, the use of highly toxic phosgene can be avoided and water is the sole byproduct.

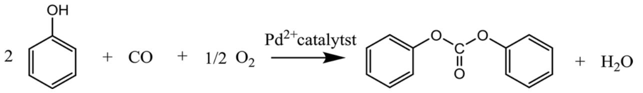

(1)

As research continues, the catalyst efficiency for the oxidative carbonylation reaction has been improved to a certain extent [6]. Homogeneous palladium catalysts $PdCl_2$, $Pd(OAC)_2$, $Pd(acac)_2$, Pd-carbene complex [7] and Pd-2,2′-bipyridyl complex [8] have been used for the oxidative carbonylation of phenol over the past few decades. Recently, heterogeneous palladium-supported catalysts have attracted more and more attention, and heterogeneous palladium catalysts anchored on various supports including activated carbon [9], polystyrene [10], silicon dioxide [11], layered double hydroxides [12], organic-inorganic hybrid materials [13] and mixed metal oxides [14,15] were extensively investigated. However, the catalyst performance is unable to meet the requirements of commercialization until now because of the fast deactivation (short lifetime) of the catalysts, which could be caused by the reduction of active palladium species during the oxidative carbonylation reaction. Therefore, it is critical to seek the solution(s) to prevent the reduction of palladium species [16]. Furthermore, it has been found that solely gaseous oxygen (O_2) is less effective at re-oxidizing the reduced palladium species than the combination of gaseous oxygen with

---

[*] Corresponding authors.
E-mail addresses: samanyan@163.com (Z. Yan), cao23@email.sc.edu (S. Cao), bin.yang@wsu.edu (B. Yang).

https://doi.org/10.1016/j.mcat.2018.07.004
Received 8 January 2018; Received in revised form 12 June 2018; Accepted 2 July 2018

the other types of oxygen species (lattice oxygen or surface oxygen) [17].

In addition to gaseous oxygen, it is necessary to verify the role of other oxygen species in the catalytic reaction. Oxygen species are proven to play a vital catalytic role in low-temperature CO oxidation, the oxidative coupling of methane, the removal of volatile organic compounds and the purification automotive exhaust gas, etc. [18]. As for oxidation carbonylation of phenol, we proposed in our previous study that 1) the formation of more OH^- group, a type of oxygen species, is more beneficial to the redox cycle between active Pd species and supports, and 2) the nature of oxygen species on the surface of a catalyst strongly depends on the metal cation (Pb^{2+}) [19]. To our best knowledge, metal doping is a typical method to alter the oxygen species in oxides. Recently, another strategy of tuning the oxygen species of catalytic material via the morphology effect in microscopic scale was reported [20–22]. Many researches have been done on the effect of morphology on metal oxide catalysts in catalytic performance, such as CeO_2, MnO_x-CeO_2 mixed oxides, etc. [23,24]. The catalytic properties of metal oxide catalysts were attributed to specific crystal planes exposed on nanocrystals with different morphology, such as the (100) planes and (110) planes exposed in cubic and rod-like CeO_2, respectively. This is because the lattice oxygen species on the (100) planes have a higher mobility than that on the (110) plane in CeO_2 [23]. Furthermore, the strong morphology-induced effect of CeO_2 on the active Pt species was observed during CO oxidation, where three morphological types of CeO_2 (cube, rod and octahedral) were employed as supports [25]. Therefore, it is essential to investigate the morphological effect of nanocatalysts and verify the role of oxygen species in the catalytic cycle of active palladium species, which would give an insight into the development of catalysts with high and stable performance.

Our research groups focused on the synthesis of Perovskite and Cryptomelane-type metal oxides as the supports for palladium catalysts [15,17,26,27]. We note that less attention is paid to the morphology of heterogeneous catalysts in the present study on the oxidative carbonylation of phenol. Herein, CeO_2 and Mn_xCe_yO mixed oxides with various morphologies were obviously synthesized by the hydrothermal method as the supports for palladium catalysts. We hope that the research on these morphological effects will provide a comparable quantitative means of deepening the fundamental understanding of the role of oxygen species in catalytic oxidative carbonylation reaction. Moreover, the interaction mechanism between the metal oxide supports and active palladium species will be explored further. Compared with morphological tuning, Mn doping was adopted to establish a more clear relationship among the oxygen species and active Pd species in terms of catalytic performance.

2. Experiments

2.1. Sample preparation

Both CeO_2 and MnO_x–CeO_2 nanomaterials were prepared under hydrothermal conditions as supports.

CeO_2 nanocubes were synthesized with a $Ce(NO_3)_3·6H_2O$ aqueous solution(3.00 g, 10 ml) and a NaOH aqueous solution (16.88 g,70 ml). The above two aqueous solutions were mixed, introduced into an autoclave, and kept at 453 K for 24 h. The precipitate from the autoclave was filtered, washed, and dried at 333 K for 6 h, and finally calcined at 673 K for 3 h. The solid obtained was denoted as CeO_2-cubes.

CeO_2 nanorods were synthesized with a $CeCl_3·7H_2O$ aqueous solution (2.99 g, 80 ml) and NaOH (38.41 g, 80 ml). The synthetic procedure of nanocubes was similar to that of the nanorods. The temperature of the autoclave was 423 K for 12 h, and the calcination temperature was 573 K for 3 h. CeO_2 nanorods are marked as CeO_2-rods.

Different amounts of $Mn(NO_3)_2$ and $MnCl_2$ were added to prepare MnO_x-CeO_2 mixed oxides with the morphology of cubes and rods based on the preparation method of pure CeO_2. The samples with the particular molar ratios of Mn to Ce of 1/3, 1/1 and 3/1 in the shape of either cubes or rods were labeled as Mn_1Ce_3O-cube, Mn_1Ce_1O-cube, Mn_3Ce_1O-cube, Mn_1Ce_3O-rod, Mn_1Ce_1O-rod, and Mn_3Ce_1O-rod, respectively.

The detailed palladium-loaded procedure of the precipitation method is as follows: $PdCl_2$ (0.42 g) was firstly dissolved in 50.0 ml of aqueous solution and the pH was subsequently adjusted to 1.0 with concentrated hydrochloric acid. The CeO_2 and MnO_x–CeO_2 supports (5.0 g) were then impregnated with the above $PdCl_2$ solution. Following that, the precipitating agent, NaOH solution (3 mol/L), was added dropwise into the above slurry until the pH value was 9–10. Finally, the supported palladium catalysts were separated by filtration and washed with distilled water several times. They were then dried at 333 K and calcined at 573 K for 3 h. The palladium supported catalysts are denoted as $Pd/Mn_xCe_yO(x,y = 1 \text{ or } 3)$ corresponding to the supports.

2.2. Characterization

X-ray Diffraction (XRD) patterns were recorded on a D8 Advance (Bruker, Germany) diffractometer using Cu Kα radiation operated at 40 kV and 200 mA, with 2θ from 10° to 80°.

Transmission Electron Microscope (TEM) images were conducted on a JEM-2100 (JEOL, Japan) operated at 200 kV, and high-resolution TEM (HRTEM) images were taken on a FEI Tecnai G2 F30 microscope operated at 300 kV. The specimen was prepared by ultrasonically dispersing the sample powder in ethanol, and droplets of the suspension were deposited on a carbon-coated copper grid and dried in air. Energy dispersive X-ray spectroscopy (EDX/EDS) was used to determine the chemical composition of the samples.

X-ray Photoelectron Spectroscopy (XPS) analysis was carried out on a K-Alpha XPS instrument (Thermo Fisher Scientific, America), employing Al- Kα radiation. The binding energy (BE) for the samples was calibrated by setting the measured BE of C 1s to 284.6 eV.

Raman Spectra were measured at room temperature using a DXR Raman microscope (Thermo Fisher Scientific, America) with a 514.5 nm excitation source from an Ar^+ laser.

Brunaur Emmett Teller (BET) nitrogen adsorption plots were used to measure the change in the specific surface area of the catalysts on a Nova 2000e surface area and pore size analyzer (Quantachrome Instruments, America).

2.3. Catalytic evaluation

The oxidative carbonylation reaction was performed in a 250 ml stainless steel autoclave equipped with a magnetic stirrer to facilitate external mass transfer. Phenol 47 g (0.5 mol), tetrabutylammonium bromide (TBAB) 1 g (3 mmol), and Pd (in the catalyst) 0.47 mmol were introduced into the autoclave. Then, the autoclave was sealed and heated to 65 °C. Subsequently, the gas mixture of CO and O_2 ($CO/O_2 = 12/1$ M ratio) became charged. After the reaction lasted for 4 h at the pressure of 4.8 MPa, the autoclave was cooled and the products were taken out. The final products were determined by capillary gas chromatography. The activity tests were carried out under a kinetic regime without the impact of mass transfer limitations.

3. Results and discussion

3.1. Morphological effects of oxide supports

The morphology of synthesized metal oxide supports was characterized by TEM, the images of which are shown in Fig. 1. The doping of Mn did not result in a change in morphology for neither nanocubes nor nanorods (Fig. 1(a)–(d)). A subtle difference that was present was that the surface of Mn_1Ce_3O-cube (Fig. 1(c)) appeared rougher and their corners were rounder than that of pure CeO_2-cube (Fig. 1(a)).